Monthly Notices of the ROYAL ASTRONOMICAL SOCIETY

MNRAS **527,** 7298–7305 (2024) https://doi.org/10.1093/mnras/stad3556
Advance Access publication 2023 November 17

Analyses of Equatorward Auroral Extensions during the Extreme Geomagnetic Storm on 15 July 1959

Hisashi Hayakawa [1,2,3,4]★ Yusuke Ebihara [5,6] and Alexei A. Pevtsov [7]

[1]*Institute for Space-Earth Environmental Research, Nagoya University, Nagoya 4648601, Japan*
[2]*Institute for Advanced Researches, Nagoya University, Nagoya 4648601, Japan*
[3]*UK Solar System Data Centre, Space Physics and Operations Division, RAL Space, Science and Technology Facilities Council, Rutherford Appleton Laboratory, Harwell Oxford, Didcot, Oxfordshire, Harwell OX11 0QX, UK*
[4]*Nishina Centre, Riken, Wako 3510198, Japan*
[5]*Research Institute for Sustainable Humanosphere, Kyoto University, Uji 6110011, Japan*
[6]*Unit of Synergetic Studies for Space, Kyoto University, Kyoto 6068306, Japan*
[7]*National Solar Observatory, 3665 Discovery Drive, 3rd Floor, Boulder, CO 80303, USA*

Accepted 2023 November 14. Received 2023 November 7; in original form 2023 September 30

ABSTRACT

Intense solar eruptions occasionally trigger extreme geomagnetic storms, expand the boundaries of the auroral oval, and facilitate equatorward extensions of the auroral visibility. It is important to analyse such events, to better understand the extremity of space weather and its impact on the technological infrastructure of the modern civilization. However, unlike other extreme geomagnetic storms, little is known about the auroral activity associated with the extreme geomagnetic storm on 15/16 July 1959, the second largest geomagnetic storm in the space age. This study acquired and analysed two Chinese accounts and one Russian account of auroral visibility at low ($\leq 40^\circ$) magnetic latitudes (MLATs). These records allowed us to conservatively reconstruct the equatorward boundaries of the auroral visibility and the auroral oval at 27.4° MLAT and 35.4° invariant latitude, respectively. Our analysis chronologically contextualized these auroral records slightly before the peak of the extreme geomagnetic storm. Moreover, their coloration indicates the excitations of, at least, nitrogen at 427.8 nm and oxygen at 557.7 nm at these low MLATs. Our results allow us to contextualize this extreme geomagnetic storm within other extreme events, based on the equatorward boundary of the auroral oval, thereby facilitating the improvement in existing empirical models for correlations of the auroral extension and the storm intensity.

Key words: Sun: coronal mass ejections (CMEs) – Sun: magnetic field – (Sun:) solar–terrestrial relations – planets and satellites: aurorae.

1 INTRODUCTION

Within the last four centuries, the late-1950s arguably witnessed the greatest enhancement of solar magnetic activity, as exemplified by the record values of sunspot number and group number around the maximum of Solar Cycle 19 (Clette & Lefèvre 2016; Svalgaard & Schatten 2016; Chatzistergos et al. 2017; Clette et al. 2023). Numerous solar eruptions and their impacts on Earth, both in terms of geomagnetic storms and solar energetic particles, have also been reported during Solar Cycle 19 (Lanzerotti 2017; Riley et al. 2018; Usoskin et al. 2020; Mursula et al. 2022). In particular, Solar Cycle 19 outnumbered other solar cycles in terms of the occurrences of geomagnetic storms (Mursula et al. 2022). This cycle hosted three of the five greatest geomagnetic storms [most negative Dst (disturbance storm time) ≤ -400 nT] and 14 of the 39 extreme geomagnetic storms (most negative Dst ≤ -250 nT) since the International Geophysical Year (1957–1958), the beginning of the space age and the Dst index (WDC Kyoto et al. 2015; Riley et al. 2018; Meng et al. 2019).

It is important to analyse such extreme geomagnetic storms, because they can considerably impact the technological infrastructure of the modern civilization, such as power grids, communication systems, and satellite operations (Lanzerotti, 2017; Baker et al. 2018; Riley et al. 2018; Oliveira et al. 2020; Hapgood et al. 2021). Fortunately, extreme geomagnetic storms occur only infrequently; however, their infrequent occurrences make their analysis challenging. Furthermore, our accelerating dependency on technological infrastructure has in turn increased our vulnerability to such extreme geomagnetic storms. Therefore, it is important to develop case studies for unique extreme geomagnetic storms, as they allow us to better understand the extremity of space weather and its potential terrestrial impacts, in combination with sophisticated models (Oliveira et al. 2020; Hapgood et al. 2021).

To this end, it is also important to understand how much the auroral oval expands under extreme space-weather events, as the expansion of the auroral electrojet triggers notable geomagnetically induced currents. Extensions of the equatorward boundary of the auroral oval

★ Email: hisashi@nagoya-u.jp

correlate well with the intensities of the related geomagnetic storm (Yokoyama, Kamide, Miyaoka 1998; Blake et al. 2021; Cliver et al. 2022). This allows us to compare modern geomagnetic storms with historical geomagnetic storms before the onset of the space age, as aurorae have been reported for millennia (Chapman 1957; Tsurutani et al. 2003; Hayakawa et al. 2019b; Knipp et al. 2021; Cliver et al. 2022).

However, it is sometimes tricky to reconstruct great auroral displays in the space age, owing to increasing urbanizations and resultant light pollutions. These developments have made it difficult to compare the auroral activity upon the space-age storms with those in the nineteenth century, as exemplified with the well-documented cases in August and September 1859 (Kimball 1960; Green & Boardsen 2006; Hayakawa et al. 2019a, 2020), October 1870 (Vaquero et al. 2008), February 1872 (Silverman 2008; Hayakawa et al. 2018), and November 1882 (Love 2018), as reviewed in several modern studies (Silverman 2006; Cliver et al. 2022; Usoskin et al. 2023).

So far, the scientific community has discussed the significant equatorward extensions of the auroral visibility and the auroral oval for the five greatest geomagnetic storms, except for the extreme geomagnetic storm on 15/16 July 1959 (most negative Dst = −429 nT) – the second greatest geomagnetic storm within the Dst index (Vallance Jones 1992; Silverman 2006; Boteler 2019; Knipp et al. 2021; Cliver et al. 2022; Hayakawa et al. 2023). In fact, the scientific community knows the equatorward expansions of the auroral oval for large magnetic storms, but little about auroral activity associated with this extreme geomagnetic storm. Therefore, this study aimed to fill this gap by analysing contemporaneous auroral reports in low (≤40°) magnetic latitudes (MLATs) for the extreme geomagnetic storm on 15/16 July 1959. We have especially focused our survey on the Chinese territory because a Chinese catalogue listed auroral visibility in Hēilóngjiāng Province on this date (Lǐ & Céng 1983). These auroral reports were analysed to reconstruct the spatial and temporal evolutions of the auroral visibility and the auroral oval during the extreme geomagnetic storm on 15/16 July 1959. Further, this study compared our reconstruction of the auroral activity with contemporaneous geomagnetic measurements to contextualize it against that of the greatest geomagnetic storms.

2 OBSERVATIONS

Two auroral reports were acquired from Chinese meteorological observatories. These reports were originally published in a Chinese magazine (*Tiānqì Yuèkān*: 天气月刊) as Céng (1960) and Féng (1960). They were later translated into English under contract by the United States Joint Publication Research Service (Tseng & Feng 1960). Another auroral account of this storm was acquired from Prof. Murzaev's travel account (Murzaev 1962). His auroral report is translated in the Appendix. Murzaev was known as a prominent Soviet/Russian physical geographer and toponymist (NB: a person who studies proper names of geographical features including their origins, meanings, usage, and types). At the time of this geomagnetic storm, he was on an expedition to Dzungaria, which lasted from 1956 to 1959. Murzaev's report is especially significant as an outdoor report during his expedition, in contrast with the other reports.

3 SPATIAL EXTENT OF AURORAL VISIBILITY AND THE AURORAL OVAL

The two Chinese auroral records describe the auroral visibility at Yīchūn (伊春; N 47°30′, E 129°20′) in Hēilóngjiāng Province (Céng 1960) and Shāndān (山丹; N 38°47′, E 101°05′) in Gānsù Province (Féng 1960). The IGRF (international geomagnetic reference field) 12 model locates the north geomagnetic pole at N 78°30′, W 069°24′ in 1959 (Thébault et al. 2015). This allows us to compute the position of geomagnetic equator and MLAT – the angular distance of the given observational site from the geomagnetic equator (see e.g. fig. 1 of Laundal & Richmond 2017). On this basis, we computed their contemporaneous MLATs as 36.5° and 27.4°, respectively.

Murzaev's auroral report (see the Appendix) was included in his travel accounts, which were written for the public (Murzaev, 1962). These accounts described travel routes taken as part of the Xīnjiāng Complex Expedition of the Academy of Sciences of the People's Republic of China, organized in close collaboration with the Soviet Academy of Sciences. Although Murzaev mentioned that his travel accounts were based on daily expedition journals, the locations of his observations could only be approximately identified. According to Murzaev (1962, p. 51), the expedition team was 'on the shores of the fast-flowing Urungu River,' 'at a latitude of 46° – the latitude of Astrakhan and the Crimea' at the night of the storm. His note provides an additional clue, stating: 'the moonlight flooded the sleeping desert with cold silver' after the auroral visibility ended. From these descriptions, Murzaev's team witnessed the auroral display somewhere in the desert on the shore of Urungu River at ≈ N 46° in latitude. Using an expedition map, we identified two desert regions along Urungu River on the expedition route (see the lower part of Fig. 1). We tentatively placed his observational site at the bend on Urungu River between these two desert areas (N 46°21′, E 088°47′), accommodating a geographical uncertainty of ≈ ±10–15 km. On this basis, we computed the MLAT as ≈35.5°.

Fig. 2 summarizes geographical distributions of the three auroral reports. These records confirm auroral visibility down to 27.4° MLAT (Shāndān). This result requires us to add this storm to the timeline of the extreme geomagnetic storms that extended auroral visibility down to < 30° MLAT, updating fig. 1 of Knipp et al. (2021) and fig. 41 of Usoskin et al. (2023), as shown in Fig. 3.

Our source records also describe the spatial extent of the auroral displays at each observational site. At Yīchūn (36.5° MLAT) on 16 July, 'the polar aurorae had reached its zenith in the sky' (Céng 1960; Tseng & Feng 1960, p. 2) by 01:45–02:05 Běijīng time (BT), which is 17:45–18:05 universal time (UT) on 15 July. Moreover, 'At 0153 h [BT on 16 July, corresponding to 17:53 UT on 15 July] suddenly there appeared six columns of white light in the zenith whose colour gave the impression of sunlight piercing through the clouds' (Céng 1960; Tseng & Feng 1960, p. 2). At Shāndān (27.4° MLAT), 'at 0230 h [BT on 16 July, corresponding to 18:30 UT on 15 July], the dark red coloured luminescent slightly increased in intensity with a corresponding enlargement of the illuminated area. At that time, its elevation [高度角] was ≈ 30°' (Féng 1960; translation modified from Tseng & Feng (1960, p. 3)). On the shore of Urungu River (35.5° MLAT), 'the flashes covered three-quarters of the sky' (Murzaev 1962, p. 51). This indicates that the auroral display extended beyond the local zenith by ≈45° along the shore of Urungu River.

Auroral visibility at any place does not immediately locate the said site directly under the auroral oval. However, we can reconstruct the equatorward boundary of the auroral oval itself, when we have geographic coordinates of the visual auroral reports with elevation angles from these sites. The equatorward boundary of the auroral oval is frequently described as invariant latitude (ILAT), the footprint of the magnetic field line along which auroral electrons precipitated [see O'Brien et al. (1962)].

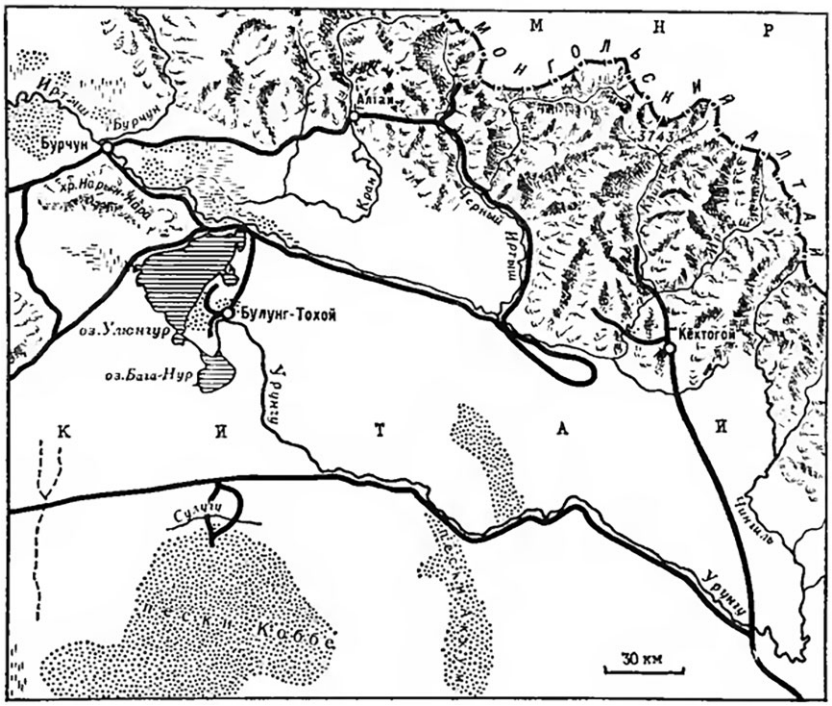

Figure 1: Xīnjiāng Complex Expedition routes (thick lines) in Dzungaria. Areas shaded with horizontal lines are lakes, the largest one being Ulungur Lake. Dotted areas mark deserts. Thin lines show rivers. Urungu River starts on the slopes of the Mongolian Altai Mountain range (on the right side of the image), makes a sharp right turn near the lower right corner of the map, continues along the expedition route (thick line), and enters the lower lake. All notations are in Russian. Reproduced from Murzaev (1973, p. 308).

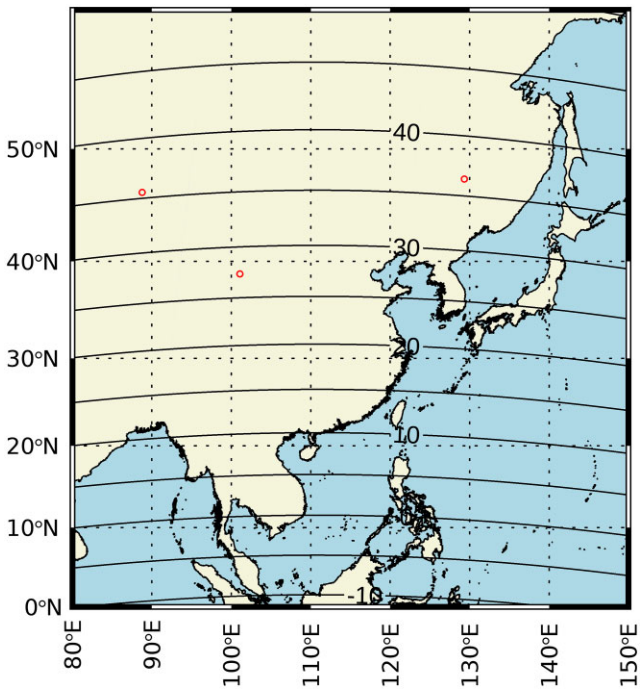

Figure 2: Geographical distributions of reported auroral visibility on 15/16 July 1959. The curves indicate the contours of the contemporaneous MLATs based on the IGRF-12 model.

The contemporaneous reports collected in this study allowed us to reconstruct the invariant latitudes (ILATs) of the equatorward boundary of the auroral oval in the extreme geomagnetic storm on 15/16 July 1959. We assumed the upper height of the visual aurora to be ≈400 km, following Roach et al. (1960) and Ebihara et al. (2017). On this basis, we computed the equatorward boundaries of the auroral emission region as 38.7° (Yīchūn), 35.4° (Shāndān), and 34.8° (Urungu) in ILATs. These estimates were broadly consistent with each other, cross-validating their reliability.

The Yīchūn report mentions not only a reddish auroral display but also pinkish light in the lower part, greenish light columns near the zenith, and light bands in the orange–yellow range. They are consistent with excitations of the nitrogen molecule ion at 427.8 nm (N_2^+), the nitrogen molecule at 670 nm (N_2), and oxygen at 557.7 nm [O I]. The orange–yellow colour is attributed to the mixture of the greenish colour of oxygen at 557.7 nm [O I] and the reddish colour of oxygen at 630.0 nm [O I]. The Shāndān report mentions that the local auroral display was predominantly in a reddish colour, with an occasional curtain structure and 'streaks of sharp red light'. These reports confirm that the reported phenomena are not stable auroral red (SAR) arcs (see Kozyra et al. 1997) but are auroral emissions with non-reddish colours and structures. In contrast, the Urungu report did not specify non-reddish colouration or explicit structures. As such, it remains unclear whether this report describes SAR arcs or auroral emissions. Therefore, it is likely more conservative to estimate the equatorward boundaries of the auroral oval and SAR arcs at 35.4° ILAT and 34.8° ILAT, respectively.

4 TEMPORAL EVOLUTION OF AURORAL ACTIVITY AND GEOMAGNETIC DISTURBANCES

Fig. 4 shows the temporal evolution of reported auroral activity during geomagnetic disturbances in the Dst index (WDC Kyoto

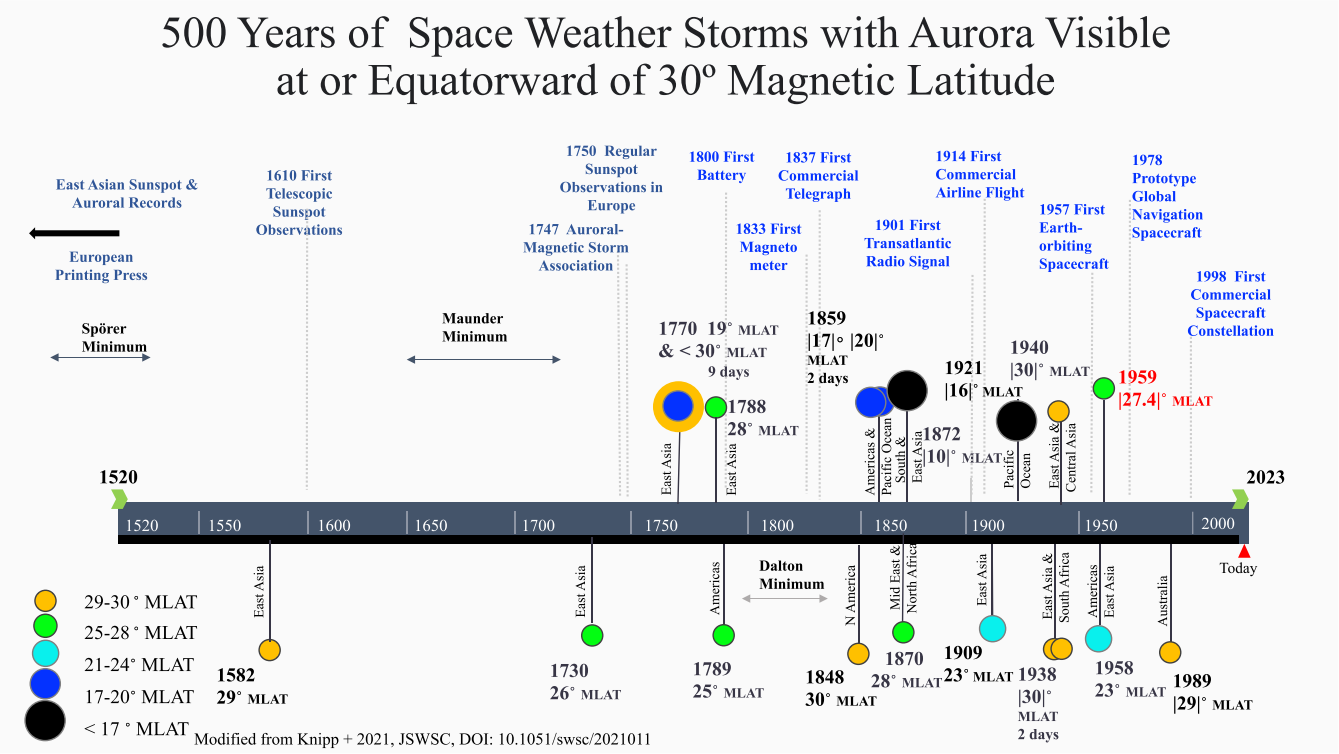

Figure 3: A revised timeline for the extreme geomagnetic storms that extended the auroral visibility beyond <30° MLAT equatorward, as modified from fig. 1 of Knipp et al. (2021) and fig. 41 of Usoskin et al. (2023). The July 1959 storm is emphasized with a reddish font.

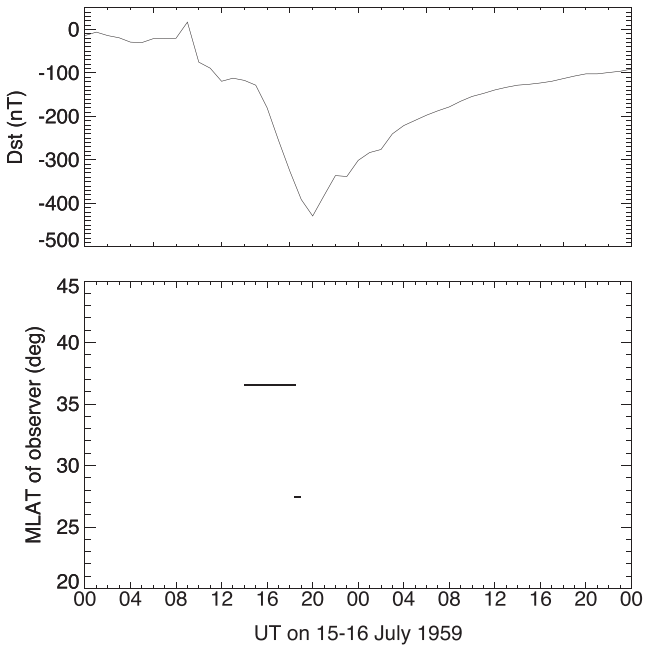

Figure 4: Duration of auroral visibility at Yīchūn (36.5° MLAT) and Shāndān (27.4° MLAT), in relation to the geomagnetic disturbances in the Dst index (WDC Kyoto et al., 2015).

et al. 2015). The Chinese reports locate the local auroral visibility at Yīchūn and Shāndān as 21:58 on 15 July to 02:31 on 16 July and 02:20–02:55 on 16 July (BT), respectively. As both of these timestamps are indicated in BT (UT + 8 h), we have converted them to the UT as follows: 13:58–18:31 (Yīchūn) and 18:20–18:55 (Shāndān) on 15 July. Fig. 4 places these auroral activities in the main phase of the storm, immediately before the storm peak at 19 UT on 15 July (most negative Dst = −429 nT).

The Yīchūn report explicitly clarifies the affection of the local dawn, stating: 'At 0215 h [BT on 16 July, corresponding to 18:15 UT on 15 July] dawn appeared in the east with the auroral light diminishing in intensity although the entire sky was still wrapped in pale pink. At 0231 h [BT on 16 July, corresponding to 18:31 UT on 15 July], the east was completely lighted, and the polar aurorae fuzzily disappeared' (Céng 1960; Tseng & Feng 1960, p. 2). This is roughly consistent with our calculations for local twilight evolution, with nautical twilight at 18:10 UT and civil twilight at 19:02 UT. In this regard, as speculated by Céng (1960) and Tseng & Feng (1960, p. 2), the local auroral activity should have continued even longer without sufficiently brightness in the dawn sky.

In Urungu, Murzaev's expedition team reported auroral visibility from 21 to 22 o'clock (Murzaev 1962, p. 51). The time zone that Murzaev used is not clear from the descriptions. Still, Murzaev hints at the presence of the Moon, stating, 'The moonlight flooded the sleeping desert with cold silver' (Murzaev 1962, p. 51). The local moonset was computed as 18:51 UT on 15 July, which is 21:51 on 15 July in Moscow Standard Time (UT + 3), 00:05 on 16 July in the local mean time, 00:10 on 16 July in Xīnjiāng Time (UT + 6), and 02:10 on 16 July in BT (UT + 8). The presence of the moon satisfies any of these choices, except for the UT hypothesis. The auroral peak time best fits the negative peak of the Dst index when we choose Moscow Standard Time (UT + 3) and convert the visibility duration to 18–19 UT; however, this calculation requires further independent verification. This uncertainty does not allow us to include this visibility duration at Urungu in Fig. 3.

Besides, auroral displays were reported in Russian stations such as Sverdlovsk (56°50′N 60°36′E) starting local midnight [see news-

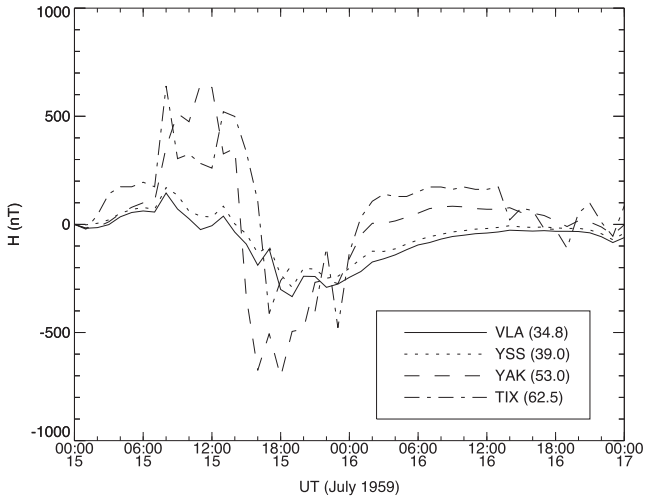

Figure 5: The disturbances of the H-component of the local geomagnetic field at Vladivostok (VLA, 34.8° MLAT), Yuzhno Sakhalinsk (YSS, 39.0° MLAT), Yakutsk (YAK, 53.0° MLAT), and Tixie Bay (TIX, 62.5° MLAT) on 15/16 July 1959.

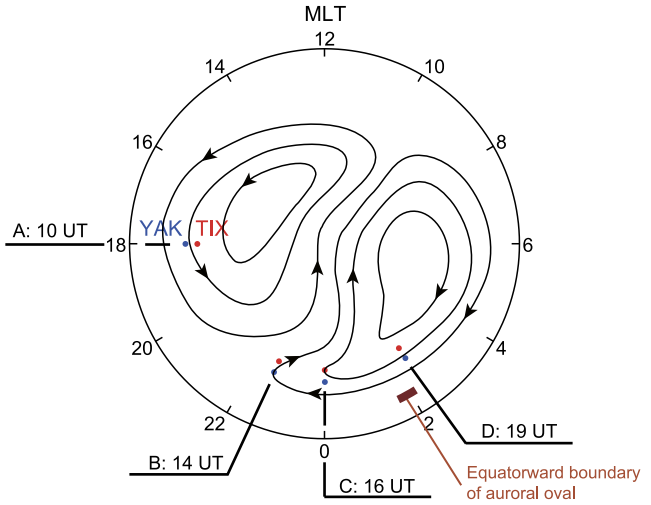

Figure 6: Schematics for possible ionospheric Hall current known as the DP2 equivalent current. The arrows indicate the direction of the Hall current. The red and blue circles indicate the positions of TIX and YAK, respectively, at 10, 14, 16, and 19 UT on 15 July 1959. The dark red arc indicates the equatorward boundary of the auroral oval.

paper clippings reproduced on Andreev (2019, p. 284)], Kirsanov[1] (52°39′N 42°44′E) during 22:10–00:20 in local time (journal entry of local meteorological station). Their visibility indicates significant auroral brightness, as these stations were under mid-summer with bright nights. Our calculation shows that the nautical twilight ended at 22:25 LT on 15 July and restarted at 02:06 LT on 16 July and the astronomical twilight lasted in between at Kirsanov. Therefore, the auroral display was bright enough to be seen under nautical twilight too.

Fig. 5 shows the disturbances of the *H*-component of the local geomagnetic field (ΔH) at Vladivostok (VLA, 34.8° MLAT), Yuzhno Sakhalinsk (YSS, 39.0° MLAT), Yakutsk (YAK, 53.0° MLAT), and Tixie Bay (TIX, 62.5° MLAT). This figure contrasts the disturbances at VLA and YSS against those at YAK and TIX. At VLA and YSS, the ΔH variations are similar to that of the Dst index and that at Kakioka. This implies that the storm-time ring current is probably the most dominant cause of the geomagnetic disturbances at these sites. At YAK and TIX, the variations are quite different from that of the Dst index and those at VLA and YSS. Therefore, the ionospheric currents (probably DP2 current) most likely flowed at these sites. Fig. 6 is a schematic showing the possible ionospheric Hall current, known as the DP2 current. The DP2 current consist of two cells. One flows in the counterclockwise direction on the duskside, and the other flows in the clockwise direction on the dawnside. From ≈ 08 to ≈ 14 UT on 15 July, ΔH is positive at YAK (MLT = UT + 8 h) and TIX (MLT = UT + 8 h), suggesting that they were located under the equatorward part of the duskside cell where the ionospheric Hall current flows in the eastward direction. Around ≈ 14 UT, ΔH turned negative (southward) at YAK, whereas it remained positive (northward) at TIX. Around ≈ 16 ut, ΔH remained southward at YAK, whereas it turned negative (southward). After that, ΔH was southward at YAK and TIX by ≈ 00 UT on 16 July. The negative turning of ΔH took place earlier at YAK than at TIX. To explain this, one solution is that the dawnside cell extends toward the duskside as shown in Fig. 6. This situation might happen when the *Y*-component of the interplanetary magnetic field is strongly positive (Foerster & Haaland, 2014). Equatorward expansion of the DP2 current should have affected the geomagnetic variations. However, the limited number of the magnetic observatories does not allow us to evaluate its effect on ΔH.

The aurora was witnessed at 13:58–18:31 UT (Yīchūn) and 18:20–18:55 UT (Shāndān). According to our estimate, the equatorward boundary of the auroral oval was located at ≈ 35.4° ILAT. During this interval, Yīchūn and Shāndān were most likely located in the equatorward part of the dawnside cell. In this region, the Hall current flows westward, meaning that eastward plasma convection occurs. It is plausible that the electrons trapped in the magnetosphere drift eastward and inward due to the enhanced convection. In the course of the drift motion, the electrons are scattered by, most likely, wave-particle interaction so as to precipitate into the upper atmosphere. The presence of the greenish light columns seen at Yīchūn may suggest that some electrons were accelerated downwardly in the direction parallel to the magnetic field. The acceleration mechanism that could take place at low latitude is uncertain. This is an important topic to be investigated in the future.

5 THE SOURCE ERUPTION(S)

The storm took place in the early decay phase of Solar Cycle 19. The Sun was still significantly spotted and eruptive enough to cause several disturbances. Fig. 7 shows solar-surface drawings in Wendelstein Observatory in mid-July 1959. These drawings show a large filament situated in the northern solar hemisphere below large active regions (especially MWO 14 284, N15 E20) close to the central meridian (N5-N12 E15-E32) on 13 July. This active region was eruptive enough to produce 76 flares, as shown in fig. 1 of Slonim (1968). Smaller filaments are located to south-west at (N8-N14 E13-E17) and north-east (N18-N23 E23-E26) of MWO 14 284 active region. However, these filaments all disappeared on 14 July, except for a small fraction of a large filament to the south of the region. These filaments seem to have erupted somewhere between the timestamps of the reports on 13 and14 July (Fig. 7).

[1]http://kirsanov-web.ru/gorod-kirsanov/kirsanovskaya-gidrometeostanciya-budni-istoriya.html?Itemid=0 , accessed on 2023 September 25, in Russian.

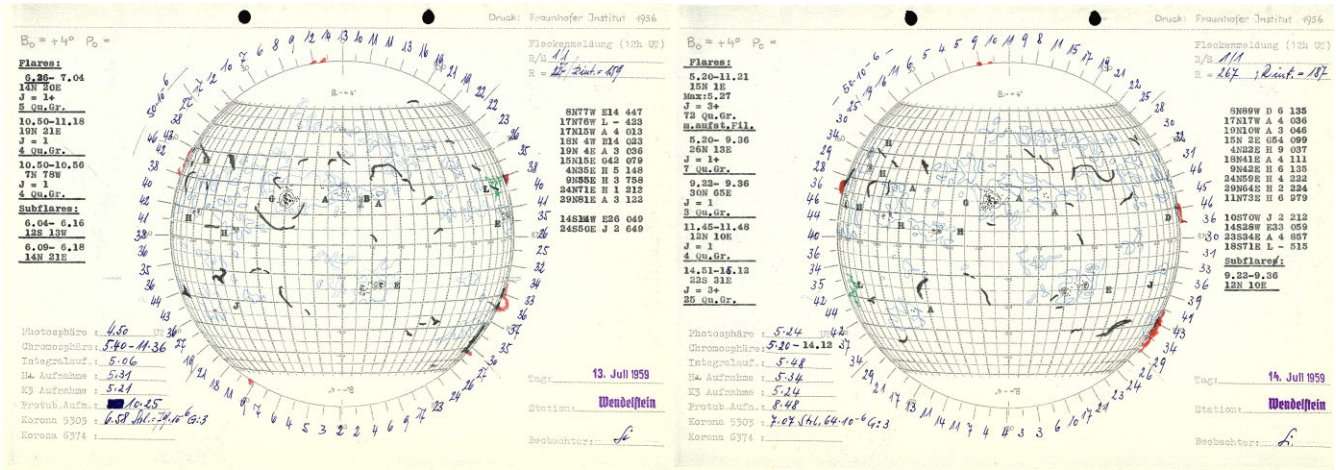

Figure 7: Whole-disc drawings for solar surface and solar filaments, as recorded in © Wendelstein Observatory on 13 and 14 July 1959.

The drawing on 14 July lists a flare of importance 3+ (in H α) with maximum at 05:27 UT at N15 E01. Below this flare report, this drawing accommodates a German annotation of '*m.ausfst.Fil.*' that is interpreted as '*mehrere Aufstieg Filaments* (several rising filaments)'. This flare was also captured in Tashkent Observatory. Slonim (1960) shows a flare profile in H α between about 03:43 UT and 04:30 UT on 14 July 1959 in her Figs 2 and 3[2] and summary table. These flare reports are probably capturing a snapshot of a gigantic and long-lasting solar flare in 03:25–11:21 UT, as observed in numerous observatories such as Nizamiah and Wendelstein (Olivieri & Lullien 1962, p. 153). This flare allowed Japanese solar radio observatories to capture solar radio bursts with their peaks at $\approx$ 03:35 UT (fig. 3 of Kodama 1962). Likewise, this solar eruption caused ionospheric disturbances at Tashkent (Slonim 1960, p. 330). This flare first caused a Dellinger effect (Sudden Ionospheric Disturbance; Weik 2000) and disrupted local connections at 03:40–04:50 UT in the 11–100 m band. Another ionospheric disturbance took place at 15:00–17:30 UT 'with complete suspension of contact at short and intermediate wavelengths (1271.2 m)' (Slonim 1960, p. 330). This chronologically coincides with the main phase of the resultant geomagnetic storm (Figs 3 and 4), indicating local development of an ionospheric storm (see also fig. 4e of Stanislawska et al. 2018).

So far, Kakioka magnetogram captured 3 SSCs (sudden storm commencements) and 2 SIs (sudden impulses) in mid-July 1959, indicating multiple arrivals of powerful interplanetary shocks around here. Among them, the source ICME for this storm arrived at $\approx$ 08:02 UT on 15 July, increasing the H component by 46 nT at Kakioka Observatory. Assuming the flare onset at 03:35 on 14 July and the ICME arrival at 08:02 on 15 July, we compute the transit time and the average velocity of this ICME as $\approx$ 28.45 h and $\approx$ 1460 km s^{-1}, respectively. This is notably a fast ICME, albeit not among the fastest category (e.g. table III of Cliver and Svalgaard 2004), which slightly modify the estimate in table 3 of Gopalswamy et al. (2005). Most probably, the preceding ICMEs cleaned up the interplanetary space and made this ICME less decelerated, as occurred in several extreme storms where multiple ICMEs cleared the interplanetary space for the subsequent ICMEs and made them even more geoeffective (e.g. Shiota & Kataoka 2016; Liu et al. 2019). This combination probably allows this specific ICME to be geoeffective enough to trigger the second greatest geomagnetic storm (most negative Dst = −429 nT) since the International Geophysical Year (IGY) that lasted from July 1957 to December 1958.

[2]Slonim's fig. 2 caption swaps the flare profiles of July 10 and July 14. However, her own table and fig. 3 confirms this swap as a mistake, in accordance with the Tashkent time profiles in the QBSA (Olivieri & Lullien 1962, p. 153).

6 SUMMARY AND DISCUSSION

In this study, we collected and analysed reports of low/mid-latitude auroral displays associated with the extreme geomagnetic storm on 15/16 July 1959. In the Dst index, this storm is known as the second strongest geomagnetic storm (most negative Dst = −429 nT) since the International Geophysical Year (1957–1958). Interestingly, the scientific community knows little about the auroral activity that occurred during this extreme geomagnetic storm, unlike those in the other four extreme geomagnetic storms that exceeded the threshold of most negative Dst = −400 nT (those in July 1957, February 1958, March 1989, and November 2003) (Vallance Jones 1992; Silverman 2006; Knipp et al. 2021; Hayakawa et al. 2023).

However, we located three sufficiently detailed mid-latitude auroral reports for this extreme geomagnetic storm. These records indicate the equatorward extension of auroral visibility to 27.4° MLAT (Shāndān), as shown in Fig. 2. The altitude profiles of these reports allowed us to conservatively reconstruct the equatorward boundaries of the auroral oval and SAR arcs down to 35.4° ILAT and 34.8° ILAT, respectively.

Our reconstructions place the auroral activity during this extreme geomagnetic storm (the second greatest geomagnetic storm since the IGY) among the most intense since the IGY (1957–1958). This reconstructed extension of auroral visibility justifies the inclusion of this extreme storm within the timeline of the great space-weather storms that extended auroral visibility equatorward beyond 30° MLAT, as shown in Fig. 3 [c.f. fig. 1 of Knipp et al. (2021) and fig. 41 of Usoskin et al. (2023)]. The reconstructed extension of the auroral oval allows us to contextualize this auroral activity upon the second greatest geomagnetic storm (most negative Dst = −429 nT) since the IGY among the greatest storms in the space age. So far, the extreme storms in September 1957 (most negative Dst = −427 nT) and February 1958 (most negative Dst = −426 nT) extended the equatorward boundary of the auroral oval to 38.3° ILAT and 33.3° ILAT, respectively, according to the visual auroral accounts (table 1 of Hayakawa et al. 2023). During the extreme storm in March 1989, the greatest geomagnetic storm in the space age (most

negative Dst = −589 nT), the auroral electron precipitations took place down to 40.1° MLAT, according to the satellite observations (Rich F., Denig W., 1992, Can. J. Phys., 70, 510).

These results also allow us to further constrain the empirical correlations between the equatorward boundaries of the auroral oval and the magnitude of the contemporaneous geomagnetic storm (Yokoyama et al. 1998; Blake et al. 2021). Based on our reconstruction (35.4° ILAT), Yokoyama et al. (1998) would estimate the storm magnitude as most negative Dst ≈ −633 nT (their fig. 3) or most negative Dst ≈ −937 nT (their figs 2 and 4). Thus, these models overestimated the intensity of extreme geomagnetic storms. In contrast, according to the most negative Dst value (−429 nT) of this storm, Blake et al. (2021) would estimate the maximal auroral extent for this storm as min 48.9° ILAT (Method 1 of their paper) or 50.4° ILAT (Method 2 of their paper). Thus, these models notably underestimated the equatorward extension of the auroral oval, as shown in this study. These discrepancies are likely caused by insufficient data availability for extreme geomagnetic storms (most negative Dst < −250 nT).

Our reconstruction of the auroral activity is also consistent with the spatial extent of the ionospheric disturbance during this storm (fig. 4e of Stanislawska et al. (2018)). This was also the case for the auroral activity in September 1957, February 1958, and November 2003, which extended auroral visibility to Japan and Greece (Knipp et al. 2021; Hayakawa et al. 2023). It would be of considerable interest to conduct further comparative analyses of auroral activity and ionospheric disturbances. Furthermore, ionospheric disturbance data indicate the needs to further investigate auroral records in West Asia, especially for auroral activity associated with the extreme geomagnetic storm on 15/16 July 1959.

ACKNOWLEDGEMENTS

We wish to thank Céng Qiángwú (曾强吾), Féng Yùjué (馮玉珏), and Eduard Makarowich Murzaev (Эдуард Макарович Мурзаев) for their valuable auroral records. HH thanks Kentaro Hattori for his advice on several contemporaneous accounts, Chiu Tinghsi (Qiū Tíngxī) and Zhū Hóngjūn for their help to access the Chinese accounts of Céng (1960) and Féng (1960), Wendelstein Observatory for allowing to access their solar records via NOAA's National Centers for Environmental Information, and staffs of the WDC for Geomagnetism at Kyoto and Kakioka Observatory for their supports to access contemporaneous geomagnetic measurements. This work was financially supported in part by JSPS Grant-in-Aids JP20K22367, JP20K20918, JP20H05643, JP20K04032, JP21H01131, JP21J00106, and JP21K13957, JSPS Overseas Challenge Program for Young Researchers, and the ISEE director's leadership fund for FY2023, Young Leader Cultivation (YLC) programme of Nagoya University, Tokai Pathways to Global Excellence (Nagoya University) of the Strategic Professional Development Program for Young Researchers (MEXT), and the young researcher units for the advancement of new and undeveloped fields, Institute for Advanced Research, Nagoya University of the Program for Promoting the Enhancement of Research Universities. HH and AAP thank the International Space Science Institute and the supported International Teams #510 (SEESUP, Solar Extreme Events: Setting Up a Paradigm), #475 (Modeling Space Weather And Total Solar Irradiance Over The Past Century), and #585 (REASSESS). HH also acknowledges the ISWAT-COSPAR S1-01 and S1-02 teams.

DATA AVAILABILITY

We have acquired the Dst index from WDC for Geomagnetism at Kyoto (WDC; Kyoto et al., 2015) and contemporaneous magnetograms from Kakioka Observatory, WDCs for Geomagnetism at Kyoto and Moscow. We have acquired whole-disc drawings for the solar surface and solar filaments in Fig. 6 from Wendelstein Observatory via NOAA's National Centers for Environmental Information (NCEI)[3].

REFERENCES

Andreev N., Андреев Н. 2019, in Тайна перевала Дятлова: все документы и главные версии о самой загадочной истории века, Komsomol'skai pravda, Russia, ISBN = 9785447003906, in Russian
Baker D. N., Erickson P. J., Fennell J. F., Foster J. C., Jaynes A. N., Verronen P. T., 2018, Space Sci. Rev., 214, 17
Blake S. P., Pulkkinen A., Schuck P. W., Glocer A., Gabor T., 2021, J. Geophys. Res. Space Phys., 126, e28284
Boteler D. H., 2019, Space Weather, 17, 1427
Céng Q.-W., 1960, Weather Monthly, **1960/6**, 47 [in Chinese]
Chapman S., 1957, Nature, 179, 7
Chatzistergos T., Usoskin I. G., Kovaltsov G. A., Krivova N. A., Solanki S. K., 2017, A&A, 602, A69
Clette F., et al., 2023, Sol. Phys., 298, 44
Clette F., Lefèvre L., 2016, Sol. Phys., 291, 2629
Cliver E. W., Schrijver C. J., Shibata K., Usoskin I. G., 2022, Living Rev. Sol. Phys., 19, 2
Cliver E. W., Svalgaard L., 2004, Sol. Phys., 224, 407
Ebihara Y., Hayakawa H., Iwahashi K., Tamazawa H., Kawamura A. D., Isobe H., 2017, Space Weather, 15, 1373
Féng Y.-J. 1960, Weather Monthly, **1960/6**, 47 [in Chinese]
Foerster M., Haaland S., 2014, J Geophys. Res. Space Phys., 120, 5805
Gopalswamy N., Yashiro S., Liu Y., Michalek G., Vourlidas A., Kaiser M. L., Howard R. A., 2005, J. Geophys. Res. Space Phys., 110, A9
Green J. L., Boardsen S., 2006, Adv. Space Res., 38, 130
Hapgood M., et al., 2021, Space Weather, 19, e2020SW002593
Hayakawa H. et al., 2018, ApJ, 862, 15
Hayakawa H. et al., 2019a, Space Weather, 17, 1553
Hayakawa H., Mitsuma Y., Ebihara Y., Miyake F., 2019b, ApJ, 884, L18
Hayakawa H., Ebihara Y., Hata H., 2023, Geosci. Data J., 10, 142
Hayakawa H., Ribeiro J. R., Ebihara Y., Correira A. P., Sôma M., 2020, Earth Planets Space, 72, 122
Kimball D. S., 1960, Sci. Rep. of Univ. Fairbanks, 6
Knipp D. J., Bernstein V., Wahl K., Hayakawa H., 2021, J. Space Weather Space Climate, 11, 29
Kodama M., 1962, J. Phys. Soc. Jpn., 17, 594
Kozyra J. U., Nagy A. F., Slater D. W., 1997, Rev. Geophys., 35, 155
Lanzerotti L. J., 2017, Space Sci. Rev., 212, 1253
Laundal K. M., Richmond A. D., 2017, Space Sci. Rev., 206, 27
Lǐ B.-G., Céng Q.-G., 1983, Bizarre Weather Phenomena, Běijīng, Qìxiàng Chūbǎnshè [in Chinese]
Liu Y. D., Zhao X., Hu H., Vourlidas A., Zhu B., 2019, ApJS, 15, 241
Love J. J., 2018, Space Weather, 16, 37
Meng X., Tsurutani B. T., Mannucci A. J., 2019, J. Geophys. Res. Space Phys., 124, 3926
Mursula K., Qvick T., Holappa L., Asikainen T. 2022, J. Geophys. Res. Space Phys., 127, e2022JA030830
Murzaev E. M., 1962, in Travel without adventure and fantasy. Geographer's Notes., Geografgiz, Moscow, 160, [in Russian]
Murzaev E. M., 1973, in Years of Research in Asia Thought Moscow 398 [in Russian]
O'Brien B. J., Laughlin C. D., van Allen J. A., Frank L. A., 1962, J. Geophys. Res., 67, 1209
Oliveira D. M., Zesta E., Hayakawa H., Bhaskar A., 2020, Space Weather, 18, e2020SW002472

[3]https://www.ngdc.noaa.gov/stp/space-weather/solar-data/solar-imagery/composites/full-sun-drawings/wendelstein/.

Olivieri G., Lullien B., 1962, Quart. Bull. Soar Activity, 9, 150
Riley P., Baker D., Liu Y. D., Verronen P., Singer H., Güdel M., 2018, Space Sci. Rev., 214, 21
Roach F. E., Moore J. G., Bruner E. C., Jr., Cronin H., Silverman S. M. 1960, J. Geophys. Res., 65, 3575
Shiota D., Kataoka R., 2016, Space Weather, 14, 56
Silverman S. M., 2006, Adv. Space Res., 38, 136
Silverman S. M., 2008, J. Atmos. Sol. Terr. Phys., 70, 1301
Slonim Y.u. M., 1960, Soviet Astron., 4, 327.
Slonim Y.u. M., 1968, Soviet Astron., 12, 225.
Stanislawska I., Gulyaeva T. L., Grynyshyna-Poliuga O., Pustovalova L. V., 2018, Space Weather, 16, 2068
Svalgaard L., Schatten K. H., 2016, Sol. Phys., 291, 2653
Thébault E., Finlay C. C., Beggan C. D., et al., 2015, Earth Planets Space, 67, 79
Tseng C.-W., Feng Y.-C., 1960, Reports of Aurora Borealis by Meteorological Stations in Communist China. Office of Technological Service Department of Commerce, Washington, D.C.
Tsurutani B. T., Gonzalez W. D., Lakhina G. S., Alex S., 2003, J. Geophys. Res. Space Phys., 108, 1268
Usoskin I. G. et al., 2023, Space Sci. Rev., 219, 73
Usoskin I., Koldobskiy S., Kovaltsov G. A., Gil A., Usoskina I., Willamo T., Ibragimov A., 2020, A&A, 640, A17
Vallance Jones A., 1992, Can. J. Phys., 70, 479
Vaquero J. M., Valente M. A., Trigo R. M., Ribeiro P., Gallego M. C., 2008, J. Geophys. Res. Space Phys., 113, A08230
WDC Kyoto, Nose M., Iyemori T., Sugiura M., Kamei T., 2015, Geomagnetic Dst Index
Weik M. H., 2000. in Computer Science and Communications Dictionary. Springer, Boston, MA
Yokoyama. N, Kamide. Y, Miyaoka H., 1998, Ann. Geophys, 16, 566

APPENDIX: THE ORIGINAL TEXT AND OUR TRANSLATION OF MURZAEV'S AURORAL REPORT

Original Text (in Russian): 15 июля 1959 года вечер застал нас на берегу быстрой Урунгу. В 9 часов тёмное небо начало как-то странно светлеть. Через несколько минут красно-малиновые сполохи окрасили северную и северо-западную части горизонта. Они на глазах стали подниматься, и скоро небосвод засветился яркими цветными красками. То было северное сияние в Центральной Азии, на широте 46°—широте Астрахани и Крыма. К 10 часам вечера сполохи охватили три четверти неба, а затем стали убывать. Краски тухли, ночь стала серой. Луна залила холодным серебром уснувшую пустыню.

Our Translation: On 15 July 1959, the evening found us on the shore of the fast-flowing Urungu River. At 9 pm, the dark sky began to brighten, somewhat strangely. A few minutes later, red-crimson flashes painted the northern and north-western parts of the horizon. They began to rise before our eyes, and soon the sky lit up in bright colours. It was the Northern Lights in Central Asia, at a latitude of 46°, the latitude of Astrakhan and Crimea. By 10 pm, the flashes covered three-quarters of the sky and then began to subside. The colours faded and the night became grey. The moonlight flooded the sleeping desert with cold silver.

This paper has been typeset from a TEX/LATEX file prepared by the author.